Propellants,
Explosives,
Pyrotechnics

Full Paper

DOI: 10.1002/prep.201(full DOI will be filled in by the editorial staff)

A computational study of density of some high energy molecules

John F. Moxnes,*[a] Finn K. Hansen,[b] Tomas L. Jensen,[a] Marta L. Sele,[a] Erik Unneberg[a]

Abstract: The detonation pressure depends quadratically on the loading density of the explosives. A precise estimate of the density is thus crucial to decide if a novel energetic material is worth pursuing. In this work we investigate theoretically the crystal densities of the energetic compounds RDX, TNT, NTO, DNAM, CL-20, DADNE, and HMX. We calculate the crystal densities by using Materials Studio 7.0 Polymorph Predictor, employing force fields and exploring molecular packing arrangements with minima in total energy. Geometry optimized molecular structures computed by density functional theory (DFT) are used as input to the density predictions. In an additional DFT study we apply two functionals, B3LYP and M06 with the 6-31G(d) and the 6-31G(d,p) basis sets, and the program package GAUSSIAN09. In this part of the work crystal densities are calculated by using the molecular isosurface volume (defined by the volume within a surface with an electron density of 0.001 electrons per Bohr^3) alone or combined with the variance of the electrostatic potential (ESP). The Polymorph Predictor seems to overestimate the densities, but the values are very dependent on the force field strength determined by charges assigned to atoms. In the GAUSSIAN09 DFT study the densities derived by using the M06 functional are in similar agreement with experimental data as what we experienced for the B3LYP results, although both functionals appear to give slightly lower densities than reported experimentally for the majority of the molecules. On average, the densities derived by the ESP method correlate equally well with measured values as the results obtained by the isosurface method.

Keywords: Density functional theory, molecular computation, explosives, crystal density, space groups

1 Introduction

Important material characteristics of high energy compounds are detonation pressure and detonation velocity. As the detonation pressure is dependent on the square of the density, an accurate knowledge of the density is important to decide the potential of a new energetic molecule. The simplest model for the crystal density ρ_{cr} assumes that the volume of a molecule is the sum of the volumes of the atoms in the molecule, but the development of the density functional theory (DFT) leads to other methods. However, due to the current inability of the DFT functionals to account for intermolecular interactions between molecules in a crystal, simulation of crystal density is not directly viable and other more indirect methods supplementing DFT are used [1]. It is notable that DFT functionals provide results that are comparable in quality with data obtained by the more elaborate *ab initio* methods, and at a fraction of the computational costs. Since no systematic approach based on the Schrödinger equation prevails, DFT functionals are constructed by educated guesses.

DFT methods may fail to predict important parameters like crystal structure and density, unless some empirical based information is given. However, a common approach for density calculations is based on the employment of three or four quantum mechanical parameters: 1) the volume within the molecular surface, where the molecular volume (isosurface volume) is defined as the volume inside the 0.001 a.u. (1 a.u. is equal to 1 electron per Bohr^3) isosurface of the electron density surrounding the molecule calculated by the DFT, 2) the area of the isosurface, 3) a measure of the variability of the electrostatic potential on the surface, 4) the degree of balance between the positive and negative charges on the isosurface [2-5].

It can be questioned whether three or four parameters of a single molecule are sufficient to determine crystal density. In a different approach, BIOVIA Materials Studio is applied to optimize the molecular structures by DFT (using the DMol^3 module [6]). The geometry optimized structures are taken into the Polymorph Predictor module where the densities are determined by Monte Carlo simulations [7]. Based on the atomic charges a force field is used for the intermolecular interactions, in this case the COMPASS force field was chosen. The approach in Polymorph Predictor is to examine possible packing arrangement for reasonable space groups to search for low-lying minima in total energy which sums intra- and intermolecular interactions. The intermolecular interactions are the sum of the molecular electrostatic energy due to charges on atoms, and the van der Waals (dispersion) interactions for our molecules. However, except for the simplest systems, the total energy surface is highly complex and depends heavily on a good estimate of the molecular electrostatic energy which is inversely proportional to the distance

[a] *J. F. Moxnes, T. L. Jensen, M. L. Sele, E. Unneberg*
Land Systems Division
Norwegian Defence Research Establishment (FFI)
P.O. Box 25, NO-2027 Kjeller, Norway
Fax: (+47) 63807509
**e-mail: john-f.moxnes@ffi.no*

[b] *F. K. Hansen*
Department of Chemistry
University of Oslo
P.O. Box 1033 Blindern, NO-0315, Oslo Norway

between point charges. Moreover, the crystal structure emerging from a particular crystallization process may be controlled by kinetics as well as thermodynamics, and the effect of the solvent on the experimental outcome of the crystallization cannot be overlooked as the solvent may modify the intermolecular interactions during the crystallization. Interestingly, Neuman *et al*. [8] used DFT and empirical van der Waals energies together with an efficient structure generator and minimizer to successfully predict four components in a blind test. See Ravi and Tewari [9] for recent density calculations based on Polymorph Predictor and Woodley and Catlow [10] for a review of different crystal structure prediction methods from first principles.

2 Theory and methods

2.1 Density

The crystal density of a compound is the mass divided by the volume. For a material of N molecules the mass is N times the molecular mass M, and the volume is N time the average volume $\overline{V}$ (molecular crystal volume). Thus, by definition the crystal density is $\rho_{cr} = NM/(N\overline{V}) = M/\overline{V}$. The objective is to construct a model for $\overline{V}$ since M is known.

The Hohenberg-Kohn existence theorem states that the ground state energy and thus all other electronic properties of a molecule are determined by the electron density $n(\vec{r})$. An important assumption for density calculations is that the crystal density (or the molecular crystal volume) is assumed to be a function of the *one* molecule electron density, to read

$$\overline{V} = \overline{V}\left[n(\vec{r})\right] \tag{1}$$

It is beneficial to define the volume and area of 'one molecule' [2-5, 11, 12]. The volume V_{iso} is defined as the volume inside the 0.001 a.u. isosurface of the electron density surrounding the molecule (isosurface volume). The isosurface is calculated quantum mechanically. The choice 0.001 a.u. of the isosurface is quite arbitrary and may depend on the chosen DFT functional. The area of a molecule A_{iso} is defined to be the area of the surface enclosing the isosurface volume and the isosurface engulfs around 99 % of the electrons.

A common method to predict the crystal density is the isosurface method, where $\overline{V}$ is assumed to be proportional to V_{iso}, *i.e.* $\overline{V} = V_{iso}/\alpha$. Here α is a constant regression parameter fitted to experiments. In fact, it has been found that α =1 gives a relatively good fit [2-4]. The density can then be calculated by Equation (2):

$$\rho_{cr} = \frac{M}{V_{iso}} \tag{2}$$

It is a major question whether this approach accounts sufficiently well for the packing of the molecule, as other parameters than the isosurface volume may also have an influence. Electrostatic interactions between neighbor molecules affect the probability of denser or less dense packing of molecules. It has been suggested that the potential (ESP) felt by a unit charge at $\vec{r}$ contains this information, to read

$$U(\vec{r}) = \sum_{nuclei\,i} \frac{Z_i}{\left\|\vec{R}_i - \vec{r}\right\|} - \int \frac{n(\vec{r}\,')}{\left\|\vec{r}\,' - \vec{r}\right\|} d\vec{r}\,' \tag{3}$$

where Z_i is the charge on nucleus i, $\vec{R}_i$ is the position of the nucleus i and $n(\vec{r})$ is the electron density of the molecule [11, 13]. The units are chosen in a way that electronic charge is -1.

Murray and coworkers [14] defined an aggregated parameter, called the balance parameter, ν, which describes the degree of positive and negative balance of the ESP on the isosurface, to read

$$\nu = \frac{\sigma_+^2 \sigma_-^2}{\left(\sigma_+^2 + \sigma_-^2\right)^2} \tag{4}$$

where σ_+^2 and σ_-^2 are defined as the variances of the positive and negative potentials on the molecule isosurface [5]. The total variance is $\sigma^2 = \sigma_+^2 + \sigma_-^2$. The Multiwfn software is used to calculate σ_+^2, σ_-^2, ν, and A_{iso} [15, 16].

The second model used to calculate the density is the ESP index method. Politzer *et al*. [5] set that $\overline{V} = V_{iso}\left(\alpha + \beta\nu\sigma^2 V_{iso}/M + \gamma V_{iso}/M\right)^{-1}$. This gives [3]:

$$\rho_{cr} = \alpha\left(\frac{M}{V_{iso}}\right) + \beta\nu\sigma^2 + \gamma \tag{5}$$

where α = 1.0462, β =0.0021 g/(cm^3(kcal/mol)^2) (*i.e.* 0.00012 g/(cm^3(kJ/mol)^2), and γ = -0.1586 g/cm^3. The geometry of the molecule was optimized at the B3LYP/6-31G(d,p) level.

Dette er en postprint-versjon / This is a postprint version.
DOI til publisert versjon / DOI to published version: 10.1002/prep.201600105

2.2 Molecules

We use three common high energy compounds (RDX, TNT and NTO) as 'benchmark' molecules. Their structures are shown in Figure 1. The other molecules in this study are DNAM, CL-20, HMX and DADNE. The structures of these energetic substances are displayed in Figure 2.

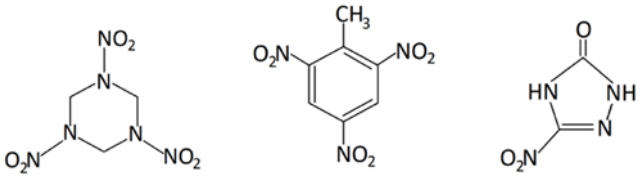

Figure 1. Molecular structures (from left to right) of 1,3,5-trinitroperhydro-1,3,5-triazine (RDX), 2,4,6-trinitrotoluene (TNT), and 3-nitro-1,2,4-triazol-5-one (NTO).

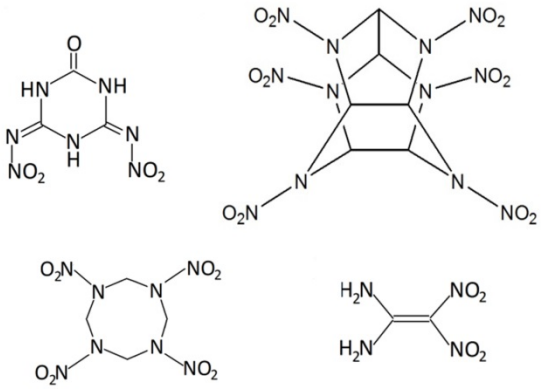

Figure 2. Molecular structures of top left: 4,6-bis(nitroimino)-1,3,5-triazinan-2-one (DNAM), top right: 2,4,6,8,10,12-hexanitro-2,4,6,8,10,12-hexaaza-isowurtzitane (HNIW or CL-20), bottom left: octahydro-1,3,5,7-tetranitro-1,3,5,7-tetrazocine (octogen or HMX), and bottom right: 1,1-diamino-2,2-dinitroethene (DADNE or FOX-7).

We also apply the isosurface and ESP methods to four other energetic molecules: [3-nitrooxy-2,2-bis(nitrooxymethyl)propyl] nitrate (pentaerythritol tetranitrate or PETN), 1,3,5-triamino-2,4,6-trinitrobenzene (TATB), 1,3,5-Trinitro-2-[2-(2,4,6-trinitrophenyl)ethenyl]benzene (hexanitrostilbene or HNS), and octanitrocubane (ONC).

2.3 Computational methods

The quantum chemical calculations are carried out by using DFT as implemented in the GAUSSIAN09 software [17].

We calculate the crystal density by using the isosurface volume (ISO) and the ESP index method. The optimized molecular structures are computed by DFT and with the B3LYP functional and the basis set 6-31G(d,p). Together with the intermolecular interactions computed by the COMPASS force field, they are used as input to the Materials Studio Polymorph Predictor to calculate the crystal densities, which are found among the low-lying minima in the total energy [7]. COMPASS is a second generation force field and should be better than the first generation force fields [18]. It is advised that consistent use of the COMPASS force field is to let COMPASS set charges on atoms. Our motivation for using this force field is that it seems to be superior to *e.g.* Dreiding, Universal, polymer consistent, and consistent-valence force fields, at least for nitramines [19].

3 Results

In Figure 3 the crystal densities calculated by various methods are compared with experimental data. The overall trend is that Polymorph Predictor overestimates the density. This is also evident from Figure 4, where calculated values are plotted against experimentally obtained densities. A straight line with slope = 1 is included in the figure to emphasize the deviations.

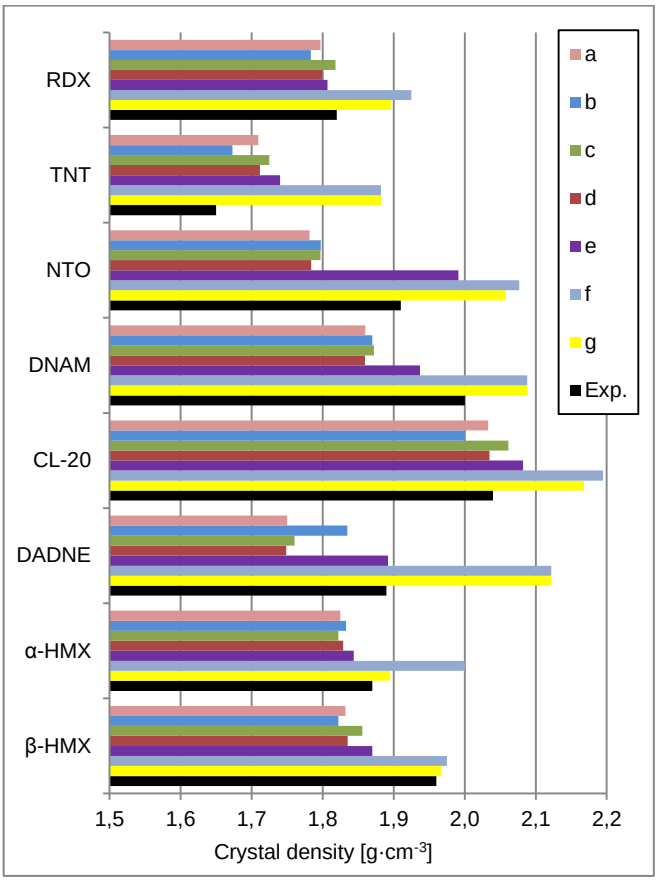

Figure 3. Calculated and experimental crystal density for various energetic molecules. a: B3LYP 6-31G(d,p) isosurface method. b: B3LYP 6-31G(d,p) ESP index method. c: M06 6-31G(d) isosurface method. d: B3LYP 6-31G(d) isosurface method. e: Polymorph Predictor, min. f: Polymorph Predictor, max. g: Polymorph Predictor, lowest total energy. Exp.: Experimental values.

Dette er en postprint-versjon / This is a postprint version.
DOI til publisert versjon / DOI to published version: 10.1002/prep.201600105

As distinct from the results above, most of the DFT calculations yield lower densities than the measured values. This finding is illustrated in Figure 3 and Figure 4. Figure 4 also contains DFT results for PETN, TATB, HNS, and ONC. Linear regression analysis of calculated *vs*. experimental densities indicates that the slope of each data set (line through the origin) is smaller than unity, but it should be kept in mind that the linearity of these relations is rather weak. For a closer inspection of the data, numerical values are listed in Table A1 (Appendix A) whereas the slope of the regression lines are given in Table A2.

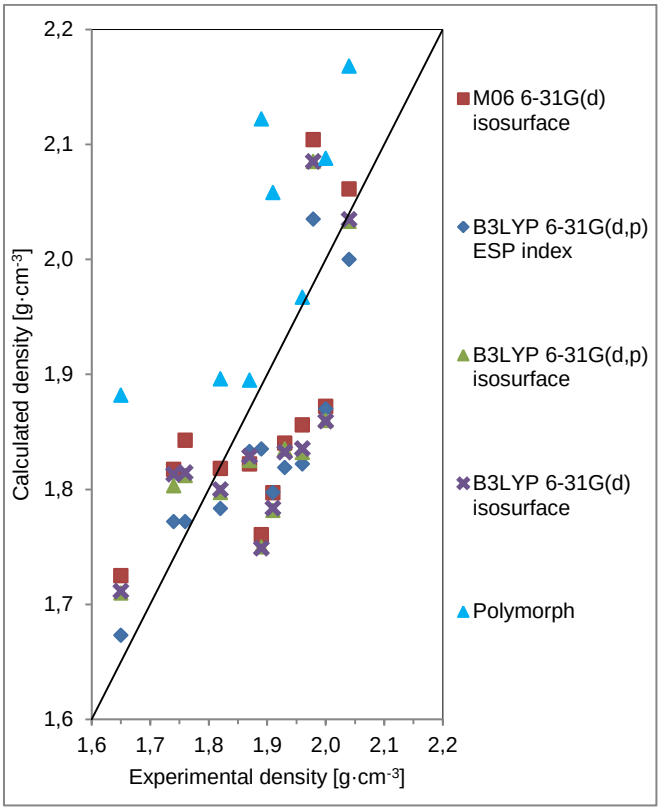

Figure 4. Calculated crystal density vs. experimental values. A straight line with slope = 1 is included in the figure.

For all molecules in our study, the B3LYP 6-31G(d,p) densities are very close to the results obtained by B3LYP 6-31G(d).

When we compare the accuracy of the ESP index method with that of the isosurface method we find (on average) no significant difference between them, although variations occur for some of the molecules. Least mean square analysis may indicate that the densities obtained by the ESP index method are slightly better fitted to the experimental values, but the mean absolute deviations are nearly equal (0.07 to 0.08 g·cm^{-3}), see Table A2 in Appendix A. These numbers are slightly higher than what was reported by Rice and Byrd [3] (0.035 g·cm^{-3}), whereas Kjønstad *et al.* [20] found an average deviation of approximately 0.05 g·cm^{-3} for their selection of molecules. It should, however, be noted that when we evaluate the precision of the computed densities we must also take the experimental data into account. For instance, the measured density of the only reported ONC polymorph is substantially smaller than the theoretical value, indicating that a denser (and yet unknown) polymorph of this molecule may exist [21].

Table 1 reveals the full set of densities derived from the various space groups by Polymorph Predictor and the optimum densities are highlighted. The differences between the highest and lowest density for each molecule are displayed in Figure 5.

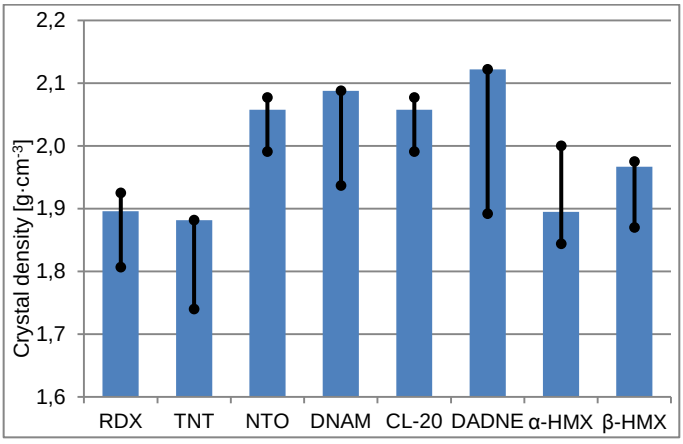

Figure 5. Crystal density calculated by Polymorph Predictor. The bars show the lowest and highest density within the space groups considered in Polymorph Predictor.

Table 1. Density (in g·cm^{-3}) for different space groups and compounds. The experimental densities are from [22] for RDX, TNT, NTO, CL-20, DADNE, and HMX. The density of DNAM is from [23]. Bold numbers show calculated density based on minimum total energy.

Space group/ molecule	C2/c (Monoclinic)	P$\bar{1}$ (Triclinic)	P2$_1$ (Monoclinic)	P2$_1$/c (Monoclinic)	P2$_1$2$_1$2$_1$ (Orthorhombic)	Pbca (Orthorhombic)	Exp.
RDX	1.881	1.894	1.807	**1.896**	1.859	1.925	1.82[a]
TNT	1.850	1.740	1.798	1.820	1.783	**1.882**	1.65[b]
NTO	2.002	2.077	2.004	**2.058**	2.036	1.991	1.91
DNAM	2.020	**2.088**	1.937	1.947	1.988	2.016	2.00[c]
CL-20	2.102	2.082	**2.168**	2.195	2.162	2.174	2.04
DADNE	2.069	2.079	2.040	2.104	**2.122**	1.892	1.89
α-HMX	**1.895**	1.844	1.967	1.930	1.899	2.000	1.87[d]
β-HMX	1.894	1.870	1.975	**1.967**	1.924	1.938	1.96[e]

[a] Pbca. [b] P2$_1$/c. [c] Pnma (orthorhombic). [d] Fdd2 (orthorhombic).

Dette er en postprint-versjon / This is a postprint version.
DOI til publisert versjon / DOI to published version: 10.1002/prep.201600105

The plots in Figures 6-13 illustrate how the minimum total (lattice) energy gives the optimum density for various crystal structures (space groups). For a given molecule, most space groups have a local optimum density near the density for the for the space group with the lowest total energy. Tables of total, van der Waals and electrostatic energy at the optimum densities are placed in Appendix B.

3.1 RDX

RDX may exist in various phases but we consider the most stable one at room temperature (α-RDX) in our work. Figure 3 shows that the DFT calculations give density results in excellent agreement with the measured density for the different DFT functionals and basis sets.

The Polymorph Predictor overestimates the density for most space groups. The minimum in total energy appears for the monoclinic $P2_1/c$ structure (Figure 6), where the calculated density of 1.896 g·cm^{-3} (Table 1) is about 3 % higher than the experimental value. For this space group our results are in good agreement with the findings of Jaidann and coworkers [24] who made use of Polymorph Predictor in an RDX study. However, the practical density measurements were carried out with RDX of the thermodynamically preferred space group Pbca. We find that the space group that gives the closest density prediction is the monoclinic $P2_1$ as we find a deviation of less than 1 %. For this space group Jaidann *et al*. [24] reported a higher density (1.89 g·cm^{-3}).

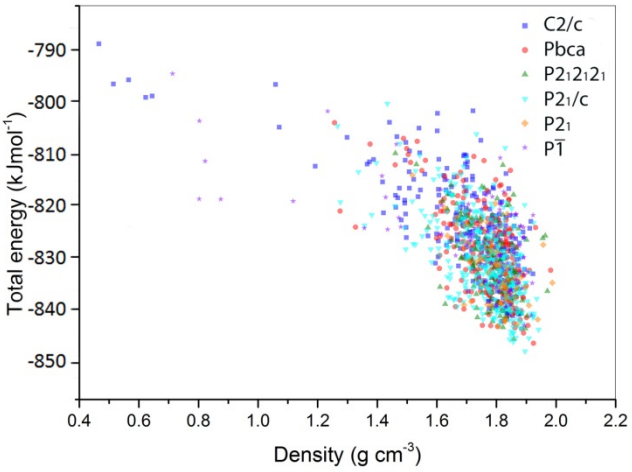

Figure 6. The total energy of RDX vs. the calculated crystal density using Polymorph Predictor.

3.2 TNT

As shown in Figure 3, the DFT methods give reasonable estimates of the density of TNT, even though they overestimate it slightly. The value calculated by the B3LYP 6-31G(d,p) ESP index method comes closest to the experimental density. A modest difference of 2 % is observed between these two results.

In contrast, the output from the Polymorph Predictor calculations is a too large TNT density. Figure 7 shows the results for different crystal structures of this molecule. The minimum in total energy is found with the orthorhombic space group Pbca, but the calculated density is 14 % higher than experienced experimentally. Table 1 reveals that the triclinic TNT structure gives the best fit when Polymorph Predictor is applied. The most stable TNT structure is the monoclinic form ($P2_1/c$), even though a metastable orthorhombic structure may exist for a period of one year or longer [25]. Our results indicate that the calculated density for the $P2_1/c$ structure is approximately 10 % higher than practical X-ray diffraction (XRD) results [26]. Therefore, the crystal structure of TNT is not well deduced from Polymorph Predictor. It should be noted that experiments have shown that the density of the monoclinic $P2_1/c$ structure is nearly equal to that of the metastable orthorhombic form [26].

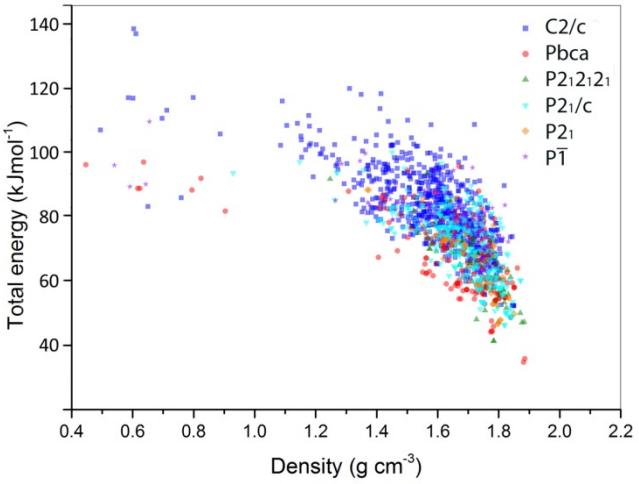

Figure 7. The total energy of TNT vs. the calculated crystal density using Polymorph Predictor.

Moreover, our calculations show that the lowest total energy (Polymorph Predictor) is positive (Table A2, Appendix A). This suggests low heat of sublimation energy for TNT and is supported by the fact that the melting point is rather low (81 °C [26]). The positive total energy indicates computational challenges.

3.3 NTO

For NTO the experimental result is 6 % higher than the theoretical results when applying the ESP or the ISO method, see Figure 3. The choice of functional does not influence the results significantly.

The density calculated by Polymorph Predictor is too large and in Figure 8 the total energy of NTO is displayed for the different crystal structures. We arrive at the minimum total energy when the space group $P2_1/c$ is applied, which is the actual crystallographic form of the β-NTO polymorph [27]. However, the more

Dette er en postprint-versjon / This is a postprint version.
DOI til publisert versjon / DOI to published version: 10.1002/prep.201600105

stable α-NTO is triclinic. The space group in Table 1 giving density closest to experiments is Pbca (orthorhombic). A deviation of approximately 5 % is observed in that case, whereas the calculated density for the $P2_1/c$ is about 8 % larger than experimentally obtained results.

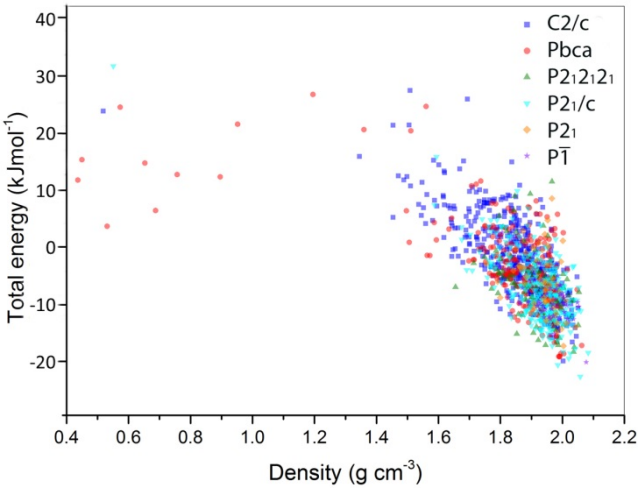

Figure 8. The total energy of NTO vs. the calculated crystal density using Polymorph Predictor.

3.4 DNAM

Compared to the experimental XRD results obtained by Simões *et al*. [23] the M06 DFT functional give too low density. A calculated value of 1.872 g·cm^3 is approximately 6 % lower than the experimental density. Applying the functional B3LYP 6-31G(d) do not lead to any improvement in this respect.

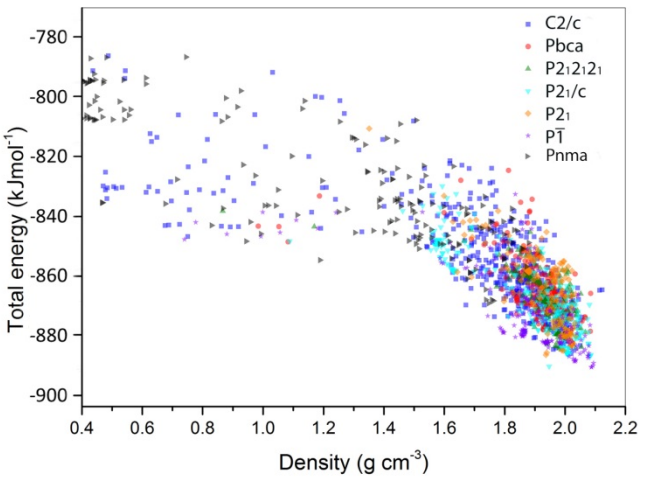

Figure 9. The total energy of DNAM vs. the calculated crystal density using Polymorph Predictor.

On the other hand, our Polymorph Predictor results overestimate the density. Based on the minimum in the total energy, we find a density that is 4 % higher than the XRD findings [23]. In addition, our result is coupled with a triclinic DNAM structure, whereas the experimental space group should be Pnma (*i.e.* orthorhombic structure). If the latter space group is chosen, the Polymorph Predictor give a density of only 1.748 g·cm^3, see Table A4 in Appendix A. The space group that gives the closest fit to the experiments performed by Simões *et al.* [23] is the orthorhombic $P2_12_12_1$. A difference of only 0.5 % is found. Figure 9 shows how the optimum space group differs.

3.5 CL-20

CL-20 may exist in four polymorphs at ambient conditions (α, β, γ and ε), where the ε phase (monoclinic, space group $P2_1/c$) is the most stable, symmetrical and dense. The DFT methods show that the calculated densities are in very good agreement with the experimental density. The isosurface method gives a nearly perfect estimate (see Appendix A).

From Table 1 it is clear that the monoclinic structure $P2_1$ gives the lowest total energy (Figure 10), but the Polymorph Predictor returns a density that is 6 % higher than the measured density of the ε polymorph. The density connected with $P2_1/c$ is calculated to be even higher, whereas the best fit is obtained for the triclinic structure.

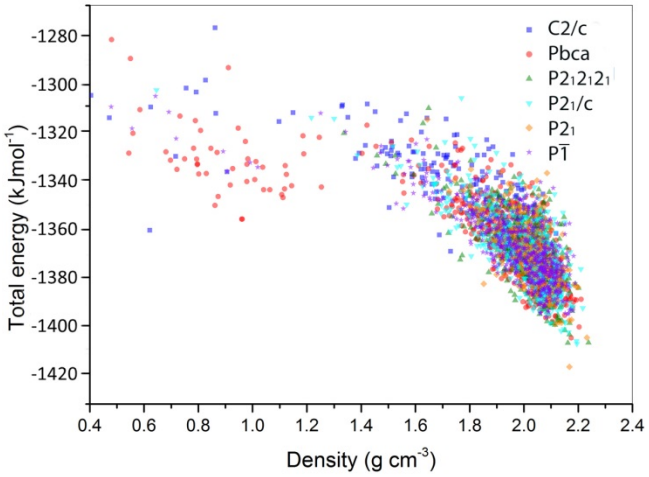

Figure 10. The total energy of CL-20 vs. the calculated crystal density using Polymorph Predictor.

3.6 DADNE

For DADNE the B3LYP and the M06 functionals show nearly the same results, but they significantly under-predict the density by approximately 7 %.

On the other hand, the DADNE density calculated by Polymorph Predictor is too high (Figure 11). We see that the van der Waals energy is positive (Appendix A), but we believe it should be negative. In detail, the orthorhombic space group $P2_12_12_1$ is the one that gave the lowest total energy, with a calculated density of 2.122 g·cm^3. Evers *et al.* [28] solved the structure for the β phase which appears at temperatures above 120 °C and found that this polymorph had the space group $P2_12_12_1$. They calculated the density to be 1.825 g·cm^3, which is lower than that of the α form. The latter has the space group $P2_1/c$ and is stable at

Dette er en postprint-versjon / This is a postprint version.
DOI til publisert versjon / DOI to published version: 10.1002/prep.201600105

ambient conditions. When this structure is basis for the Polymorph Predictor, we obtain a density that is 11 % higher than the experimental value. The best similarity between measured and calculated vales is achieved for the orthorhombic space group Pbca.

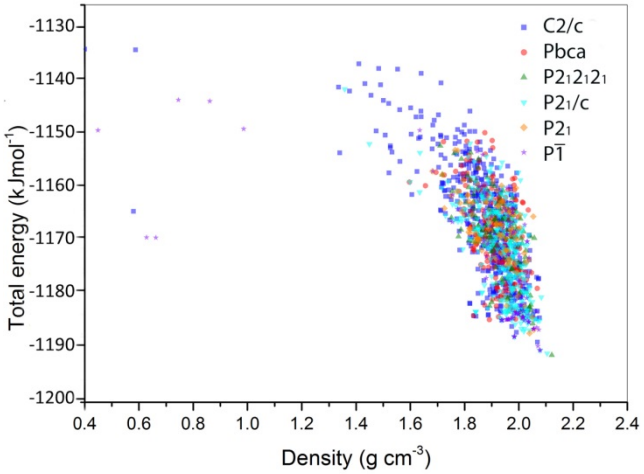

Figure 11. The total energy of DADNE vs. the calculated crystal density using Polymorph Predictor.

3.7 HMX

HMX may appear in several phases, and in this work we draw our intention towards the most stable one at room temperature, β-HMX. We do also include the α phase, which is stable in the temperature region 115-156 °C [26]. We find that the DFT calculations give a density that is about 2 % smaller than the experimental density, whereas the difference is larger (5-6 %) for β-HMX. The results obtained by B3LYP are close to the M06 densities. For β-HMX, the M06 functional is slightly better than the B3LYP functional, but the functionals give similar estimates for the α-HMX density.

The Polymorph Predictor results for β-HMX are in good agreement with experimental findings, and the calculations for the α phase do also give a good value for the density, even though this result does not address the same space group (Figure 12 and Figure 13). In all these calculations the NO_2 groups are modeled by either one single and one double bond between the two oxygen atoms and the nitrogen atom or by two one and a half bonds, as this is a resonance structure. However, it is not self-evident that this is the best representation for the NO_2 group. If we use two double bonds in the structure, the calculated density is significantly lower because the charges on the atoms in the NO_2 group are altered. The electrostatic energy is sensitive to charges on atoms since they influence the force field strength and the more negative the electrostatic energy, the higher the density for a given compound. It is advised that consistent application of the COMPASS force field with its parameters is to let the force field also define the charges on the atoms instead of using the charges calculated by DFT. The latter would probably be more accurate, but the COMPASS force field is optimized for a number of experimentally measured physical properties and consistent use of this force field makes it possible to assign both inter- and intramolecular parameters. A result of this is that in the NO_2 group the net charge is zero when using COMPASS.

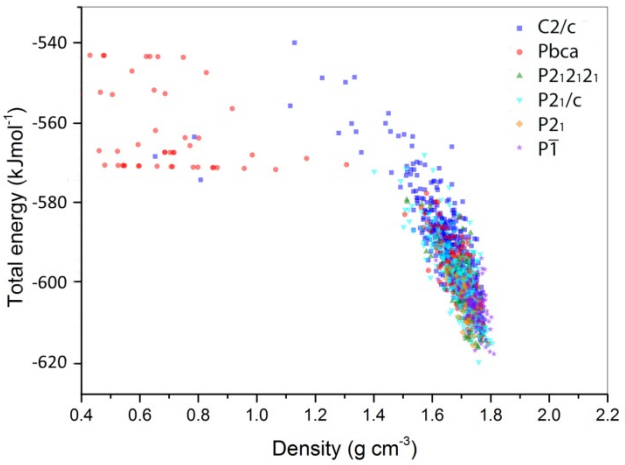

Figure 12. The total energy of α-HMX vs. the calculated crystal density using Polymorph Predictor.

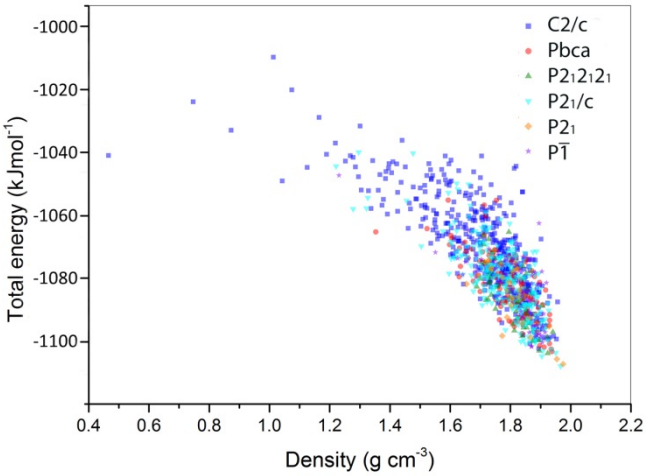

Figure 13. The total energy of β-HMX vs. the calculated crystal density using Polymorph Predictor.

For HMX additional calculations using the charges calculated by the DFT functional are carried out. These charges are shown to be marginally different in α-HMX and β-HMX because of the slight variation in the intra-atomic interactions caused by the difference in steric atomic positions. In this case the charges on the NO_2 group do not sum to zero and the total energies of α-HMX and β-HMX are positive, but differ by approximately 120 kJ·mol^{-1}. The positive total energies show that using charges assigned by DFT are not useful when the COMPASS force field is applied. Further studies are necessary to reveal the exact charge on atoms of α- and β-HMX. These charges strongly influence the density and thus the impact sensitivity.

Dette er en postprint-versjon / This is a postprint version.
DOI til publisert versjon / DOI to published version: 10.1002/prep.201600105

4 Discussion and Conclusion

We have made a theoretical study of the crystal density of some high energy compounds where the three common compounds RDX, TNT, and NTO were used as benchmark molecules. In addition, we have examined the molecular explosives DNAM, CL-20, DADNE and HMX in a similar way.

Polymorph Predictor calculations gave HMX densities in good agreement with reported experimental values. That was, however, not the case for the other molecules in this study, as their densities were overestimated by 8 % on average. Densities obtained by Polymorph Predictor are very dependent on the force field strength determined by the atomic charges, and variations in the charges strongly influence the electrostatic energy which again influences density. The more negative the electrostatic energy, the higher the density for a given compound. A much larger set of compounds should be examined to see whether the viability of the Polymorph Predictor can be increased.

For most of the molecules in this study the DFT methods calculated the densities better than the Polymorph Predictor. The mean absolute deviation from measured densities was 4 % and the majority of the computed values were slightly lower than the measured densities. On average, the M06 functional results were in about the same agreement with the experimental values as the densities obtained by B3LYP. Furthermore, our calculations carried out with the functional B3LYP 6-31 G(d,p) were very close to the densities computed with B3LYP 6-31 G(d).

All methods require a well suited DFT functional to give a satisfactory prediction of the density.

Symbols and Abbreviations

B3LYP – Hybrid DFT functional

CL-20 – 2,4,6,8,10,12-Hexanitro-2,4,6,8,10,12-hexa-azaisowurtzitane

DADNE – 1,1-Diamino-2,2-dinitroethene

DFT – Density Functional Theory

DNAM – 4,6-Bis(nitroimino)-1,3,5-triazinan-2-one

ESP or U(r) – Electrostatic potential

HNS – 1,3,5-Trinitro-2-[2-(2,4,6-trinitrophenyl)ethenyl]benzene

HMX – Octahydro-1,3,5,7-tetranitro-1,3,5,7-tetrazocine

ISO – Molecular isosurface volume

M06 – Hybrid DFT functional

$n(\vec{r})$ – Electron density

NTO – 3-Nitro-1,2,4-triazol-5-one

ONC – Octanitrocubane

PETN – [3-Nitrooxy-2,2-bis(nitrooxymethyl)propyl] nitrate

$\vec{R}_i$ – Position of nucleus i

RDX – 1,3,5-Trinitroperhydro-1,3,5-triazine

TATB – 1,3,5-Triamino-2,4,6-trinitrobenzene

TNT – 2,4,6-Trinitrotoluene

$\overline{V}$ – Average molecular volume

V_{iso} – Volume within the isosurface

Z_i – Charge on nucleus i

XRD – X-ray diffraction

ν – Degree of balance between the positive and the negative electrostatic potentials on the isosurface

ρ_{cr} – Crystal density

σ^2 – Total variance of the electrostatic potential on the isosurface

σ_-^2 – Variance of the negative electrostatic potential on the isosurface

σ_+^2 – Variance of the positive electrostatic potential on the isosurface

References

[1] L. Goerigk, S. Grimme, A Thorough Benchmark of Density Functional Methods for General Main Group Thermochemistry, Kinetics and Noncovalent Interactions, *Phys. Chem. Chem. Phys.* **2011**, 13, 6670-6688.

[2] B. M. Rice, J. J. Hare, E. F. C. Byrd, Accurate Predictions of Crystal Densities Using Quantum Mechanical Molecular Volumes, *J. Phys. Chem.* **2007**, 11, 10874-10879.

[3] B. M. Rice, E. F. C. Byrd, Evaluation of the Electrostatic Descriptors for Predicting Crystalline Density, *J. Comput. Chem.* **2013**, 34, 2146-2151.

[4] Chan Kyung Kim, Soo Gyeong Cho, Chan Kon Kim, Hyung-Yeon Park, Hui Zhang, Hai Whang Lee, Predictions of Densities of Solid Energetic Molecules with Molecular Surface Electrostatic Potentials, *J. Comput. Chem.* **2008**, 29, 1818-1824.

[5] P. Politzer, J. Martínez, J. S. Murray, M. C. Concha, A. Toro-Labbé, An Electrostatic Interaction Correction for Improved Crystal Density Prediction, *Mol. Phys.* **2009,** 107, 2095-2101.

[6] B. Delley, An All-Electron Numerical Method for Solving the Local Density Functional for Polyatomic Molecules, *J. Chem. Phys.* **1990**, 92, 508-517 and B. Delley, From Molecules to Solids with the $DMol^3$ Approach, *J. Chem. Phys.* **2000**, 113, 7756-7764.

[7] Accelrys Software Inc., Materials Studio, Release 7.0, San Diego, **2014**.

[8] M. A. Neumann, F. J. J. Leusen, J. Kendrick, A Major Advance in Crystal Structure Prediction. Angew. Chem. Int. Ed. **2008**, 47, 2427-2430.

[9] P. Ravi, S. P. Tewari, A DFT Study of Tautomers of 3-amino-1-nitroso-4-nitrotriazol-5-one-2-oxide, *J. Mol. Model.* **2013**, 19, 2539-2547.

Dette er en postprint-versjon / This is a postprint version.
DOI til publisert versjon / DOI to published version: 10.1002/prep.201600105

[10] S. M. Woodley, R. Catlow, Crystal Structure Prediction from first Principles, *Nat. Mater*. **2008**, 7, 937-946.

[11] J. S. Murray, P. Politzer, Statistical Analysis of the Molecular Surface Electrostatic Potential: an Approach to Describing non-Covalent Interactions in Condensed Phases, *J. Mol. Struct.*, **1998**, 425, 107-114.

[12] P. Politzer, J. Martínez, J. S. Murray, M. C. Concha, An Electrostatic Correction for Improved Crystal Density Predictions of Energetic Ionic Compounds, *Mol. Phys.* **2010**, 108, 1391-1396.

[13] J. S. Murray, T. Brinck, P. Politzer, Relationships of Molecular Surface Electrostatic Potentials to some Macroscopic Properties, *Chem. Phys*. **1996**, 204, 289-299.

[14] J. S. Murray, P. Lane, T. Brinck, K. Paulsen, M. E. Grice, P. Politzer, Relationships of Critical Constants and boiling points to Computed Molecular Surface Properties, *J. Phys. Chem*. **1993**, 97, 9369–9373.

[15] Tian Lu, Feiwu Chen, Multiwfn: A Multifunctional Wavefunction Analyzer, *J. Comp. Chem.* **2012**, 33, 580-592.

[16] Tian Lu, Feiwu Chen, Quantitative Analysis of Molecular Surface Based on Improved Marching Tetrahedra Algorithm, *J. Mol. Graph. Model*. **2012**, 38, 314-323.

[17] Gaussian 09, Revision A.02, M. J. Frisch, G. W. Trucks, H. B. Schlegel, G. E. Scuseria, M. A. Robb, J. R. Cheeseman, G. Scalmani, V. Barone, B. Mennucci, G. A. Petersson, H. Nakatsuji, M. Caricato, X. Li, H. P. Hratchian, A. F. Izmaylov, J. Bloino, G. Zheng, J. L. Sonnenberg, M. Hada, M. Ehara, K. Toyota, R. Fukuda, J. Hasegawa, M. Ishida, T. Nakajima, Y. Honda, O. Kitao, H. Nakai, T. Vreven, J. A. Montgomery, Jr., J. E. Peralta, F. Ogliaro, M. Bearpark, J. J. Heyd, E. Brothers, K. N. Kudin, V. N. Staroverov, R. Kobayashi, J. Normand, K. Raghavachari, A. Rendell, J. C. Burant, S. S. Iyengar, J. Tomasi, M. Cossi, N. Rega, J. M. Millam, M. Klene, J. E. Knox, J. B. Cross, V. Bakken, C. Adamo, J. Jaramillo, R. Gomperts, R. E. Stratmann, O. Yazyev, A. J. Austin, R. Cammi, C. Pomelli, J. W. Ochterski, R. L. Martin, K. Morokuma, V. G. Zakrzewski, G. A. Voth, P. Salvador, J. J. Dannenberg, S. Dapprich, A. D. Daniels, O. Farkas, J. B. Foresman, J. V. Ortiz, J. Cioslowski, D. J. Fox, Gaussian, Inc., Wallingford CT, **2009.**

[18] H. Sun, COMPASS: An ab Initio Force-Field Optimized for Condensed-Phase Applications - Overview with Details on Alkane and Benzene Compounds, *J. Phys. Chem. B* **1998**, 102, 7338-7364.

[19] P. B. Kempa, M. Herrmann, Molecular Mechanical Simulations of Nitramines: A Comparison of Force Fields, *42nd Int. Annual Conference of ICT*, Karlsruhe, Germany, June 26 - July 1, **2011**, p. 81.1–81.20.

[20] E. F. Kjønstad, J. F. Moxnes, T. L. Jensen, E. Unneberg, A Critical Investigation of Proposed Electrostatic Corrections to Quantum Mechanical Volumes: The Importance of Variation and the Irrelevance of Imbalance, *Mol. Phys*. **2016**, 111, 1822-1830.

[21] P. E. Eaton, M.-X. Zhang, R. Gilardi, N. Gelber, S. Iyer, R. Surapaneni, *Octanitrocubane: A New Nitrocarbon*, Propellants Explos. Pyrotech. **2002**, 27, 1.

[22] R. Meyer, J. Köhler, A. Homburg, Explosives, 6th edition, Wiley-VCH Verlag GmbH, Weinheim, **2007**.

[23] P. N. Simões, L. M. Pedroso, A. M. Matos Beja, M. Ramos Silva, E. MacLean, A. A. Portugal, Crystal and Molecular Structure of 4,6-Bis(nitroimino)-1,3,5-triazinan-2-one: Theoretical and X-ray Studies. *J. Phys. Chem. A* **2007**, 111, 150-158.

[24] M. Jaidann, L-S. Lussier, A. Bouamoul, H. Abou-Rachid, J. Brisson, Effects of Interface Interactions on Mechanical Properties in RDX-Based PBXs HTPB-DOA: Molecular Dynamics Simulations, in: *Computational Science – ICCS 2009, 9th International Conference, Baton Rouge, LA, USA, May 25-27, 2009. Proceedings, Part II* (Eds.: G. Allen, J. Nabrzyski, E. Seidel, G. D. van Albada, J. Dongarra, P. M. A. Sloot), Springer, Berlin **2009**, pp. 131-140.

[25] R. M. Vrcelj, J. N. Sherwood, A. R. Kennedy, H. G. Gallagher, T. Gelbrich, Polymorphism in 2-4-6-Trinitrotoluene, *Cryst. Growth Des*. **2003**, 3, 1027-1032.

[26] G. R. Miller, A. N. Garroway, *A Review of the Crystal Structures of Common Explosives. Part I: RDX, HMX, TNT, PETN, and Tetryl,* Naval Research Laboratory, Washington, DC 20375-5320, NRL/MR/6120—01-8585, **2001.**

[27] M. W. Smith, M. D. Cliff, *NTO-Based Explosive Formulations: A Technology Review*, Report DSTO-TR-0796, DSTO Aeronautical and Maritime Research Laboratory, Salisbury, Australia, **1999**.

[28] J. Evers, Thomas M. Klapötke, P. Mayer, G. Oehlinger, J. Welch, α- and β-FOX-7, Polymorphs of a High Energy Density Material, Studied by X-ray Single Crystal and Powder Investigations in the Temperature Range from 200 to 423 K, *Inorg. Chem.* **2006**, 45, 4996–5007.

Dette er en postprint-versjon / This is a postprint version.
DOI til publisert versjon / DOI to published version: 10.1002/prep.201600105

Appendix A

In Table A1 the densities obtained by DFT and various functionals are listed. Experimental values are included in the table. Figure 3 and Figure 4 are based on these data.

Table A1. Crystal densities (in g·cm^{-3}) determined by various methods.The experimental densities are literature values.

Molecule	M06 6-31G(d) isosurface	B3LYP 6-31G(d,p) ESP index	B3LYP 6-31G(d,p) isosurface	B3LYP 6-31G(d) isosurface	Exp.
RDX	1.818	1.783	1.797	1.800	1.82[a]
TNT	1.725	1.673	1.710	1.712	1.65[a]
NTO	1.797	1.797	1.782	1.784	1.91[a]
DNAM	1.872	1.870	1.860	1.859	2.00[b]
CL-20	2.061	2.000	2.033	2.035	2.04[a]
DADNE	1.761	1.835	1.750	1.749	1.89[a]
α-HMX	1.822	1.833	1.825	1.829	1.87[a]
β-HMX	1.856	1.822	1.832	1.835	1.96[a]
PETN	1.843	1.772	1.812	1.815	1.76[a]
TATB	1.840	1.819	1.835	1.832	1.93[a]
HNS	1.817	1.772	1.803	1.813	1.74[a]
ONC	2.104	2.035	2.085	2.085	1.98[c]

[a] Ref. [22]. [b] Ref. [23]. [c] Ref. [21].

In a plot of calculated vs. experimental densities we find that the linear regression line through the origin is smaller than unity for the DFT values, whereas it is larger than unity when Polymorph Predictor is applied. The slopes of the regression lines are listed in Table A2. The mean absolute deviations between calculated and measured densities are included in the table.

Table A2. Slope of regression line and mean absolute deviation for crystal densities determined by various methods.

	M06 6-31G(d) isosurface	B3LYP 6-31G(d,p) ESP index	B3LYP 6-31G(d,p) isosurface	B3LYP 6-31G(d) isosurface
Slope	0.988	0.975	0.981	0.980
Mean absolute deviation [g·cm^{-3}]	0.08	0.07	0.08	0.08

Appendix B

This appendix shows the density and energy of different compounds. The unit of energy is kJ·mol^{-1}. The unit of density is g·cm^{-3}.

Table B1. Density and energy of RDX.

Space group	Density	Total energy	van der Waals energy	Electrostatic energy
$P2_1/c$	1.896	-848.56	-19.37	-809.98
Pbca	1.925	-846.97	-21.05	-806.55
$P2_12_12_1$	1.859	-846.21	-16.90	-810.44
$P2_1$	1.807	-843.75	-10.59	-812.45
$P\bar{1}$	1.894	-843.62	-18.62	-804.79
C2/c	1.881	-843.49	-18.33	-806.59

Table B2. Density and energy of TNT.

Space group	Density	Total energy	van der Waals energy	Electrostatic energy
Pbca	1.882	35.61	-1.00	32.84
$P2_12_12_1$	1.783	42.17	-4.90	41.67
$P2_1/c$	1.820	47.03	-0.67	44.10
$P2_1$	1.798	47.49	-5.36	47.32
C2/c	1.850	53.18	-3.64	53.43
$P\bar{1}$	1.740	63.51	-4.52	59.25

Table B3. Density and energy of NTO.

Space group	Density	Total energy	van der Waals energy	Electrostatic energy
$P2_1/c$	2.058	-22.59	-47.82	-24.10
$P\bar{1}$	2.077	-20.08	-48.12	-23.05
C2/c	2.002	-19.83	-45.69	-23.89
Pbca	1.991	-19.12	-46.19	-22.59
$P2_12_12_1$	2.036	-18.28	-47.78	-21.17
$P2_1$	2.004	-17.24	-46.40	-21.97

Table B4. Density and energy of DNAM.

Space group	Density	Total energy	van der Waals energy	Electrostatic energy
$P\bar{1}$	2.088	-890.56	-68.66	-505.68
$P2_1/c$	1.947	-890.31	-62.09	-510.07
$P2_1$	1.937	-886.42	-64.48	-504.97
C2/c	2.020	-886.05	-68.70	-502.46
$P2_12_12_1$	1.988	-884.71	-65.90	-502.62
Pbca	2.016	-883.74	-70.17	-495.55
Pnma	1.748	-869.14	-64.64	-489.57

Table B5. Density and energy of CL-20.

Space group	Density	Total energy	van der Waals energy	Electrostatic energy
$P2_1$	2.168	-1417.46	-32.47	-1413.36
$P2_1/c$	2.195	-1407.79	-39.92	-1401.01
$P2_12_12_1$	2.162	-1407.41	-36.61	-1402.10
Pbca	2.174	-1405.28	-27.78	-1410.43
$P\bar{1}$	2.082	-1396.58	-32.17	-1405.20
C2/c	2.102	-1391.93	-33.51	-1396.58

Table B6. Density and energy of DADNE.

Space group	Density	Total energy	van der Waals energy	Electrostatic energy
$P2_12_12_1$	2.122	-1191.90	0.33	-1056.38
$P2_1/c$	2.104	-1191.56	2.38	-1057.67
$P\bar{1}$	2.079	-1190.98	4.35	-1059.31
C2/c	2.069	-1189.43	4.94	-1056.21
$P2_1$	2.040	-1187.75	4.77	-1054.91
Pbca	1.892	-1185.16	3.85	-1054.16

Table B7. Density and energy of α-HMX.

Space group	Density	Total energy	van der Waals energy	Electrostatic energy
C2/c	1.895	-1108.05	-24.43	-1063.57
$P2_1/c$	1.930	-1107.97	-25.65	-1062.65
$P2_1$	1.967	-1106.17	-32.97	-1053.57
$P2_12_12_1$	1.899	-1103.74	-28.03	-1062.02
Pbca	2.000	-1102.86	-37.36	-1047.72
$P\bar{1}$	1.844	-1099.68	-23.68	-1057.59

Dette er en postprint-versjon / This is a postprint version.
DOI til publisert versjon / DOI to published version: 10.1002/prep.201600105

Table B8. Density and energy of α-HMX, calculated with two double bonds in the NO_2 group.

Space group	Density	Total energy	van der Waals energy	Electrostatic energy
$P2_1/c$	1.759	-619.65	-84.77	-406.31
$P\bar{1}$	1.811	-617.64	-91.63	-405.43
$P2_12_12_1$	1.756	-616.09	-86.65	-399.95
$P2_1$	1.740	-615.47	-81.17	-402.67
Pbca	1.792	-615.09	-92.55	-400.58
C2/c	1.764	-614.00	-85.56	-402.21

Table B9. Density and energy of β-HMX.

Space group	Density	Total energy	van der Waals energy	Electrostatic energy
$P2_1/c$	1.967	-1107.34	-31.80	-1062.15
$P2_1$	1.975	-1106.67	-24.69	-1071.82
$P2_12_12_1$	1.924	-1103.24	-28.28	-1058.80
Pbca	1.938	-1102.74	-30.54	-1058.80
C2/c	1.894	-1101.73	-23.56	-1063.91
$P\bar{1}$	1.870	-1101.15	-22.51	-1063.99

Received: ((will be filled in by the editorial staff))
Revised: ((will be filled in by the editorial staff))